In-field Plant Phenotyping using Multi-view Reconstruction: An Investigation in Eggplant

Thuy Tuong Nguyen[1], David C. Slaughter[1], Brad T. Townsley[2], Leonela Carriedo[2], Julin N. Maloof[2], Neelima Sinha[2]

[1]Department of Biological and Agricultural Engineering, [2]Department of Plant Biology, University of California, Davis, CA 95616, USA

A paper from the Proceedings of the
13th International Conference on Precision Agriculture
July 31 – August 4, 2016
St. Louis, Missouri, USA

Abstract. *Rapid methods for plant phenotyping are a growing need in agricultural research to help accelerate improvements in crop performance in order to facilitate more efficient utilization of plant genome sequences and the corresponding advancements in associated methods of genetic improvement. Manual plant phenotyping is time-consuming, laborious, frequently subjective, and often destructive. There is a need for building field-deployable systems with advanced sensors that have both high-speed and high-performance for plant phenotype processing.*

This study reports on the design and performance of a new 3D computer vision-based plant phenotyping technology that utilizes 3D stereovision from many different viewing angles. The research presents new knowledge used to facilitate the determination of the best viewing angles for 3D reconstruction of plants. A full 3D reconstruction system for plants is introduced that utilizes 16 high-resolution color stereovision cameras mounted on an arc-shaped superstructure designed for in-field use. The system incorporates both unique hardware features (including multiple cameras per arc and structured illumination to enhance the visual texture of plant surfaces) and software algorithms (including 3D feature extraction of plant height, number of leaves, leaf area, and plant biomass). Results demonstrate the ability to reconstruct complete 3D models of the plants growing in the natural outdoor environment of a farm. The system allows photo-realistic plant models to be

created from an optimum (i.e. minimum) number of digital color cameras positioned at different viewing angels. Experimental results of comparisons between different sets of viewing angles reveal that the top views are most advantageous for small plants while the side views provide greater information content for larger plants, where top views are detrimental in estimating plant height due to plant main stem occlusion by top leaves.

Keywords. *Plant phenotyping, multi-view reconstruction, 3D reconstruction, performance evaluation, 3D feature extraction, angle of view, point cloud.*

Introduction

Plant phenotyping [Dhondt 2013, Furbank 2011] is an important aspect of plant breeding used in the agricultural research and seed industry to help improve crop productivity through modern techniques of genetic improvement. Manual methods of plant phenotyping are frequently destructive, time-consuming, and laborious. When destructive methods, such as the harvest of foliage to determine leaf area, are used it does not allow monitoring the same plant during growth over time. The knowledge of how plants are affected by environmental condition changes during growth is important to breeders to improve the understanding of plant genetics as related to plant performance in reaction to climate change, for example. To address these deficiencies, there is a need for building field-deployable systems with advanced sensors that have rapid and accurate performance in plant phenotype measurement and processing.

Color cameras are the advanced sensors that have been extensively utilized in agricultural automation for their high resolution, efficiency, and low cost when compared to other sensors [Song 2014, Slaughter 2006, Nguyen 2015(1), Nguyen 2015(2), Grift 2011]. Recent camera-based methods have been developed for 3D modeling and phenotyping of plants, leaves, and fruits. A structured light based 3D reconstruction and phenotyping system for small plants was introduced in [Nguyen 2015(1)] with the ability to precisely estimate the number of leaves, leaf size, plant height, and internode distance. Non-destructive automatic leaf area measurements were presented [Song 2014] with a combination of the stereo and time-of-flight (ToF) images. The study [Paproki 2012] introduced a novel 3D mesh-based method for temporal high-throughput plant phenomics. By utilizing the 3D S.O.M. software [Baumberg 2005] for 3D scanning, this study provided mesh segmentation, phenotypic parameter estimation and plant organ tracking over time to obtain high accuracies of leaf size and stem height. A low-cost, low-resolution stereovision camera (Kinect, Microsoft Co., Redmond, WA, USA) sensor [Zhang 2012] was used to provide depth information-based leaf segmentation and measurement of plant height in an indoor environment [Chene 2012]. A plant phenotyping system was introduced in [Heijden 2013] to automatically measure characteristics of tall pepper plants in the greenhouse. This system was equipped with ToF and color cameras to support the plant height over three meters, and to have 3D reconstruction based extraction of leaf size and angle.

Several studies have investigated the best camera viewing angles and accuracy of analysis for multiple view based plant phenotyping. In [Rose 2015], 3D reconstruction based estimations of main stem height, leaf area, and convex hull were evaluated and a comparison between using a laser scanner and a digital single-lens reflex camera with commercial structure-from-motion software were conducted. All experimental images were taken from standing positions (without camera holders), at a tilt angle of approximately 45° downwards from the horizontal, and at a height of 50 cm over the plant's top point. This study reported that an overlap of 70% between two successively acquired images had to be maintained during the image acquisition process for satisfactory 3D reconstruction using their method. In [Andujar 2015], an indoor stereovision camera (Kinect, Microsoft Co., Redmond, WA, USA) was utilized to find the best camera viewing angle to estimate plant biomass, plant height, and leaf area in an indoor environment. Four different angles of view were evaluated and compared in this study: inferior (from below looking upwards) perspective view (-45°), superior (downwards view from above) perspective view (45°), top view (0°), and front view (90°). This work concluded that 1) top views yielded inferior results because of the fact the bottom leaves were

occluded by the top leaves, 2) small plants were better estimated from the top view, and 3) the front view showed it was one of the best locations for taller trees. Additionally, data evaluation for 3D reconstruction of buildings was presented in [Koutsoudis 2014]. This study quantified the quality of the structure-from-motion data with the ToF terrestrial 3D range scanner data by performing distance measurements between feature points on the monument's surface. However, there is lack of a completely accurate analysis model for the best viewing angles where multiple cameras are mounted fixed on a 360° frame surrounding the target plant. Even though it is possible to have full reconstruction and characterization of plants, satisfactory results are occasionally unattainable or the reconstruction is time-expensive due to many highly overlapped views.

This paper presents an accuracy evaluation of 3D based plant phenotyping with different number of cameras distributed at different viewpoints. In our outdoor plant phenotyping system, 16 high-resolution color digital cameras are spatially distributed in the upper hemisphere above the plant, at four different height levels. This system is a version of the indoor system of [Nguyen 2015(1)], that has been further refined for outdoor use in agricultural row crops, specifically vegetables. For the purpose of evaluation of plant phenotyping at different camera view angles, structure-from-motion techniques are utilized in this study instead of stereo vision as presented in [Nguyen 2015(1)]. Our accuracy evaluation considers that the camera position is a key factor because some plant features could be miscalculated due to an incorrect capturing angle between the camera and the target plant. The 16-viewpoint system was designed to optimize the camera capturing angles to the plant (to minimize the miscalculation of plant features) and image overlap (to minimize the time for 3D feature matching and reconstruction). The purpose of this study is to assess the spatial distribution for stereovision cameras which are fixed to a stationary frame for superior modeling of plants under outdoor field conditions. Eggplants are chosen as target plants in this work because of their large leaves causing high occlusion rate, which strongly requires multiple camera views.

Materials and Methods

System design

The image data of individual plants were collected by 16 electronically controlled, high-resolution, digital single-lens reflex cameras (Model EOS Rebel T3, Canon Inc., Tokyo, Japan). These cameras, each equipped with a zoom lens (Model EF-S 18–55 mm 1:3.5–5.6 IS II, Canon Inc., Tokyo, Japan), were mounted on four different arms (located at 0°, 90°, 180°, and 270°, see Figure 1) in a tractor-drawn structure and were all aimed at the target plant. Each group of four cameras was held fixed relative to one another on a support arm located at 80°, 60°, 40°, and 20° relative the ground plane. Figure 1 shows the mechanical structure of our system, where Figure 1B shows the layout of camera positions on the four arms and at four height levels: top cameras were at a height of approximately 130 cm, middle-top cameras at 110 cm, middle-bottom cameras at 90 cm, and bottom cameras at 70 cm above the ground plane, respectively. Each camera was mounted vertically and translated on the arm with a distance of approximately 25 cm relative to the next one in order to optimize the overlap between their images. All cameras were connected to a remote switch to allow the cameras to be fired exactly at the same time, which was important for in-field activities in order to minimize plant motion between images associated with wind. The entire system was additionally covered by translucent plastic panels to provide indirect illumination and manage wind. All 16 color images, each with a resolution of 4272 × 2848 pixels, were captured in the field and processed offline using a computer. Camera parameters (focal length, exposure time, aperture, white balance, ISO, and image stabilization) were selected to provide the best quality images for 3D feature matching and reconstruction of eggplant.

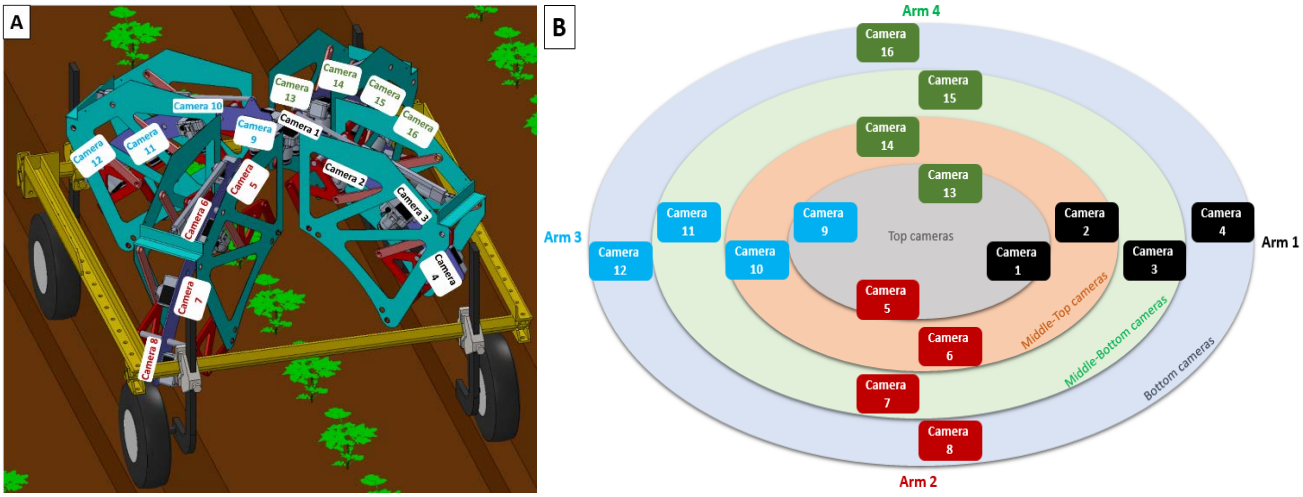

Fig 1. Sketch of the mechanical structure (A) of the UC Davis outdoor plant phenotyping system and spatial distribution of the 16 cameras (B) which are supported by four arms at 0°, 90°, 180°, and 270° and four height levels: top (at 80° and 130 cm height), middle-top (at 60° and 110 cm height), middle-bottom (at 40° and 90 cm height), and bottom (at 40° and 70 cm height).

A structured light, supplemental illumination system, consisting of five light sources, was adapted from [Nguyen 2015(1), Nguyen 2016(1)] and used in this study to provide plant-stationary visual texture enhancement of plant foliage from all camera viewpoints. Each structured illumination module utilized a telephoto 105-mm focal length lens (Model NIKKOR-P f/2.5, NikonCo., Tokyo, Japan) with a high-power, 29-mm diameter LED array (Model BXRC-40E10K0-L-03, Bridgelux Inc., Livermore, CA, USA, white color, maximum 10,000 luminous flux and correlated color temperature of 4000 K), designed to project grayscale, random-dot patterns printed in high resolution on clear film onto the scene. One structured light was mounted on top of the four-arm structure to project structured light from above the scene, and the other four lights were located between each pair of adjacent camera support arms. The random-dot patterns were created using a 3000 × 3000 pixel grayscale image with a printed resolution of 1200 dots-per-inch, where a 30% Hurl noise was applied to a transparent background. This projected pattern was designed to support the 3D matching algorithm at a three pixel-wide resolution of approximately 1 mm on the leaf surface of a plant. Figure 2 shows an example set of 16 images of a single eggplant growing outdoors, taken simultaneously by the 16 cameras in the system in Figure 1.

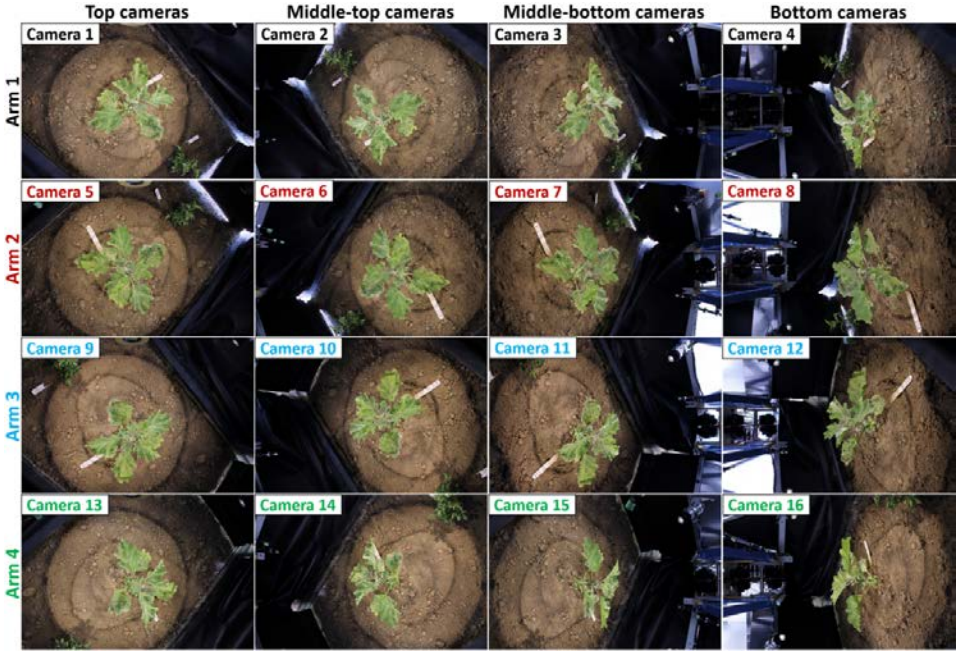

Fig 2. Images of an eggplant seedling taken by the UC Davis in-field 3D plant phenotyping system.

Software algorithms

A computer software method was developed to translate the 16 individual images of each plant into a 3D model of the plant from which plant architecture phenotypes could be extracted. The software was organized in two major steps. First, a 3D reconstructed model of the target plant was determined using a structure-from-motion software (PhotoScan [Agisoft PhotoScan 2016] was utilized). This software was used to perform the initial 3D visual feature extraction and matching steps needed to align visual features within the 16 images with high accuracy, and to create a dense, robust 3D point cloud of the objects in the scene with very high precision. In the second step, phenotyping features were extracted from the 3D point cloud output obtained in the first step using algorithms customized for eggplant. To evaluate the accuracy of plant phenotyping using visual information acquired from different viewing angles, the software process in step one was executed sequentially using separate subsets of top, middle-top, top and middle-top, top and middle-bottom, top and bottom, middle-top and middle-bottom, middle-top and bottom, top and middle-top and middle-bottom, top and middle-top and bottom, top and middle-bottom and bottom, middle-top and middle-bottom and bottom, and all images. Figure 3 shows an example of the 3D reconstruction model results for the plant shown in Figure 2 using the sequence of the image subsets captured from different camera viewpoints. A 3D region of interest containing the target plant, but eliminating the phenotyping equipment visible in the 3D point cloud, obtained from step one, was automatically extracted based on its distance to the cameras.

In this study, parameters of both mechanical structure and software algorithms were fixed and adapted for all data to optimize the phenotyping performance. In the structure-from-motion software (PhotoScan), the "*Align Photos*" parameters were set as *Accuracy: High*, *Pair preselection: Disabled*, *Key point limit: 20,000,000*, and *Tie point limit: 100,000*. The *Quality* and *Depth filtering* parameters in the "*Build Dense Cloud*" step were defined *High* and *Disable*, respectively. Our implementation required the parameters set as: clustering tolerance is 0.002, minimum cluster size is 2500, leaf size threshold $T_{size} = 0.001$, leaf direction threshold $T_{direction} = 0.82$, and leaf position threshold ratio is 0.4.

Custom algorithms were developed to estimate plant height, the number of leaves, leaf area, and plant biomass in eggplant from the 3D point cloud data. Prior to plant feature extraction, the region of interest in the 3D point cloud was transformed to the space where its X, Y, Z axes fit to the original coordinates, based on eigenvector calculation. The transformed point cloud was then clustered into smaller portions so that the plant features could be efficiently estimated. The Euclidean based method was used for point cloud clustering by making use of 3D grid subdivision with fixed width boxes [Rusu 2009].

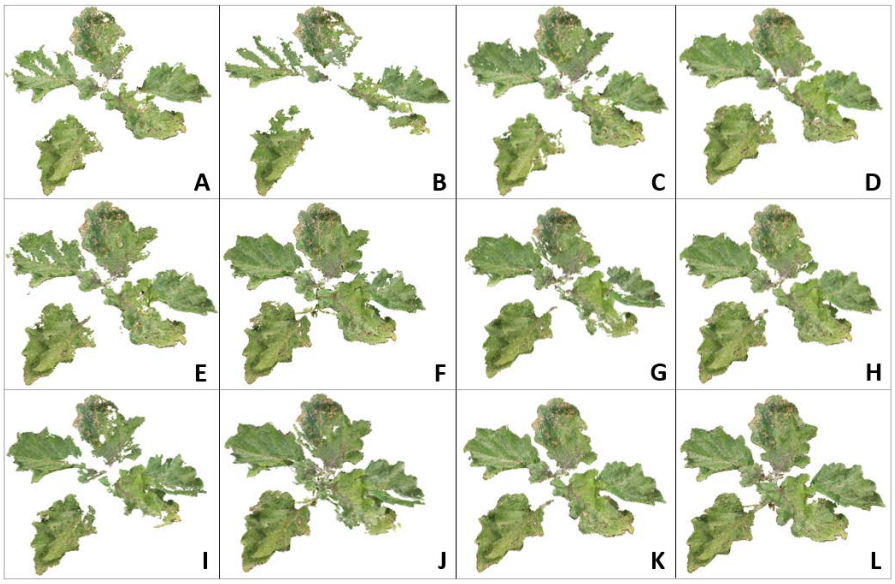

Fig 3. Reconstruction results of (A) Top, (B) Middle-top, (C) Top and Middle-top, (D) Top and Middle-bottom, (E) Top and Bottom, (F) Middle-top and Middle-bottom, (G) Middle-top and Bottom, (H) Top and Middle-top and Middle-bottom, (I) Top and Middle-top and Bottom, (J) Top and Middle-bottom and Bottom, (K) Middle-top and Middle-bottom and Bottom, and (L) All images.

Estimation of plant height

Plant height was determined as the absolute Z-difference of the maximum and minimum 3D coordinates within the entire point cloud.

Estimation of the number of leaves

Referring the leaf detection method in [Nguyen 2015(1)], a cluster was determined as a leaf if its maximum eigenvalue was greater than a threshold T_{size}, the magnitude of its dominant direction should not be much larger than that of other directions (as defined through a threshold $T_{direction}$), and it had to be above a ratio of the plant height, otherwise the cluster is not counted as a leaf.

Estimation of leaf area

To estimate leaf area, a 3D bounding box of each leaf had to be determined based on the leaf centroid and eigenvectors. Product of the 3D bounding box's length and width was considered the leaf area.

Estimation of plant biomass

Unlike the ideal point cloud results obtained using laser scanners in [Paulus 2014, Calders 2015], our camera based results had some parts that were mismatched or not detected successfully in the steps of structure-from-motion. Typically, small parts were not shown in the final point cloud and this led to a reduction in the accuracy of plant feature extraction. Therefore, the conventional methods for plant volume convex hull [Paulus 2014, Costes 2008] and allometric equations based plant biomass estimation [Calders 2015, Paul 2013], applied to the laser scanning generated point clouds, were not utilized in this study. Instead, a plant biomass estimation method, described in this section based on plant main stem diameter, plant height, and total leaf volume, was developed. Equations to estimate the above-ground biomass for plants were defined as linear equivalent forms:

$$B = (V_L + V_{MS}) \times r_B,$$

where B is the plant biomass, V_L is the total volume of all detected leaves (i.e. the total volume of 3D leaf bounding boxes), r_B is the biomass ratio to convert a point cloud unit to a real-world unit, and VMS is the volume of plant main stem which was calculated as

$$V_{MS} = [\pi \times (D_{MS} / 2)^2] \times [H_p \times r_{MS}],$$

where D_{MS} is main stem diameter, H_p is plant height, and r_{MS} is a ratio of main stem height to the plant height H_p. According to the experimental data, described in later sections, the mean main stem diameter, D_{MS}, of the plants in this study was determined to be 0.87 cm based on the average measurement of the ground-truth data. In the same manner, the main stem height ratio r_{MS} was determined to be 0.92 in our study. The biomass ratio, r_B, defined as 0.05, was also used as a parameter to compensate for the difference between leaves and their bounding boxes, and miss detection of petioles.

All processing steps were done on a computer (CPU Model Core i7 at 3.4 GHz, Intel Co., Santa Clara, CA, USA, with 12-GB DDR3 random-access-memory) with an 1152-core GPU (Model GeForce GTX 760, NVidia Co., Santa Clara, CA, USA) graphics card which was used for fast feature extraction and dense point cloud reconstruction.

Validation experiment

The 3D reconstructed parameters were validated by comparison with manual measurements made on the actual plants in the field (for plant height and biomass) and by 2D photography (for leaf area) using a digital camera (model Olympus SP-500UZ, Olympus Co., Tokyo, Japan). Prior to photography, the leaves were arranged on a photographic background after they were harvested from the plant, and a glass panel was placed on top of them to flatten them with minimal leaf folding. Barrel distortion of the images taken by the Olympus camera was corrected manually using image processing software (GNU Image Manipulation Program [GIMP 2016]). Leaf areas of the reference leaves were carried out using a ruler-based mapping from a pixel unit to a real-world unit using image processing software (ImageJ [ImageJ 2016]). For the number of leaves and leaf area, only the leaves having widths and lengths longer than 2.5 cm were considered. Reference plant heights were manually measured as the distance from the top point to the most bottom point of the plant, right above the ground. Root mean square errors (RMSE) and mean absolute percentage errors (MAPE) were calculated using the measurements of point clouds, measurements of manual method, and the number of measurements.

Results and discussion

The average processing time for 3D reconstruction was approximately 2, 6, 10, and 15 minutes for 4, 8, 12, and 16 camera views, respectively. Less than half a second was required for the software implementation of the steps performing cropping the originally reconstructed point cloud, projecting the cropped cloud to the origin, and calculating 3D features. Eight eggplant plants were investigated in this section. These plants were chosen as examples of plants with various plant heights (from 13.97 to 30.48 cm), numbers of leaves (from 4 to 10 leaves), leaf areas (from 264.04 to 1641.23 cm^2), plant biomasses (from 13.1 to 100.4 gram), curved leaves, touching leaves, high density of leaves, and small leaves attached to the main stem. Table 1 shows a list of the experimental plants with their height, number of leaves, total leaf area, and biomass.

Table 1. List of the eight eggplant plants with their manual measurements used for the experiments.

	Height (cm)	Number of leaves	Total leaf area (cm^2)	Biomass (g)	Brief description
Eggplant 1	19.69	7	713.09	45	Curved, touching leaves at top, small leaves at bottom
Eggplant 2	10.79	4	264.04	13.1	Curved leaves at top, less leaf touching
Eggplant 3	13.97	6	461.96	24.4	Curved leaves at top, small leaves occluded by top leaves
Eggplant 4	15.69	6	577.01	35.6	Big, curved leaves, less small leaves
Eggplant 5	22.86	8	1058.11	55.6	Curved, touching leaves, different size of leaves
Eggplant 6	20.96	6	946.99	48.3	Curved leaves, good separation between leaves
Eggplant 7	27.31	10	1593.88	100.4	High density of leaves, small leaves attached to main stem
Eggplant 8	30.48	10	1641.23	87.9	Good separation between leaves

The high resolution of the 16-camera system allowed phenotyping of plants on the basis of plant morphology, i.e. plant height and leaf area. The complete 3D point cloud was used to derive the parameters for the complete plant. Figure 4 shows the determination of the plant height of eight eggplants in 12 different sets of camera viewpoints. The *All* set, having images from 16 different vantage points, yielded the best results (R^2 0.936, slope 0.891, RMSE 2.11, and MAPE 8.65), while the Middle-top (*MT*) set was the worst (R^2 0.326, slope 0.252, RMSE 14.45, and MAPE 73.69). The Middle-top, Middle-bottom, Bottom (*MT*+*MB*+*B*) and Top, Middle-top, Middle-bottom (*T*+*MT*+*MB*) sets, based on images from 12 different vantage points, had results approximately as good as the *All* set. The unsatisfactory plant height estimations from the other sets of viewpoints was due to the fact that large leaves covered the main stem at the plant bottom which required more views from the side of the plant to mitigate. Notice that the target plant was cropped out from the soil ground, so there was no other reference points except the plant itself. According to the results, the top views did not allow good estimation of the plant height.

Figure 5 presents the validation results for the estimate of the number of leaves. Generally, all sets, except the *MT* set, produced acceptable estimation of leaf count, even though small bottom leaves were occluded by the top leaves in the top views. Promising leaf detection, with RMSE values of 0.5, 0.61, 0.71, 0.79, and 1 (in the unit of the number of leaves), was obtained from the sets having more than 12 camera views: *All*, *MT*+*MB*+*B*, *T*+*MT*+*MB*, *T*+*MB*+*B* (Top, Middle-bottom, Bottom), and *T*+*MT*+*B* (Top, Middle-top, Bottom), respectively. Moreover, taller eggplants had better leaf detection rates than shorter plants because leaf occlusion and touching between adjacent leaves was reduced. In Figure 6, a set of 56 leaves, with leaf areas from 11.84 to 290 cm^2, from the eight plants were plotted. There were 10 small leaves having areas lower than 50 cm^2, 13 leaves from 50 to 100 cm^2, 9 leaves from 100 to 150 cm^2, and 24 big leaves having areas from 150 to 290 cm^2. The 16-image set showed good leaf area measurement potential with a sufficiently small MAPE of 8.26%. Summing up all the sizes of the individual plant parts, the total phenotype parameters of the whole plant could be calculated (e.g. total leaf area). Accuracy evaluation for the total leaf area parameter is presented in Figure 7.

Above-ground plant biomass estimates were compared to the harvested reference measures in Figure 8. The biomass estimate from the 3D point cloud was generally below the actual measured value. The cases of *T*+*MT*+*MB*, *T*+*MT*+*B*, *MT*+*MB*+*B*, and *All* images yielded highly accurate results with RMSE values of 3.26, 4.57, 7.04, and 4.04 (in the unit of gram), respectively. The *MT* set had a very large MAPE at 59.64%, the worst of the various viewpoint sets.

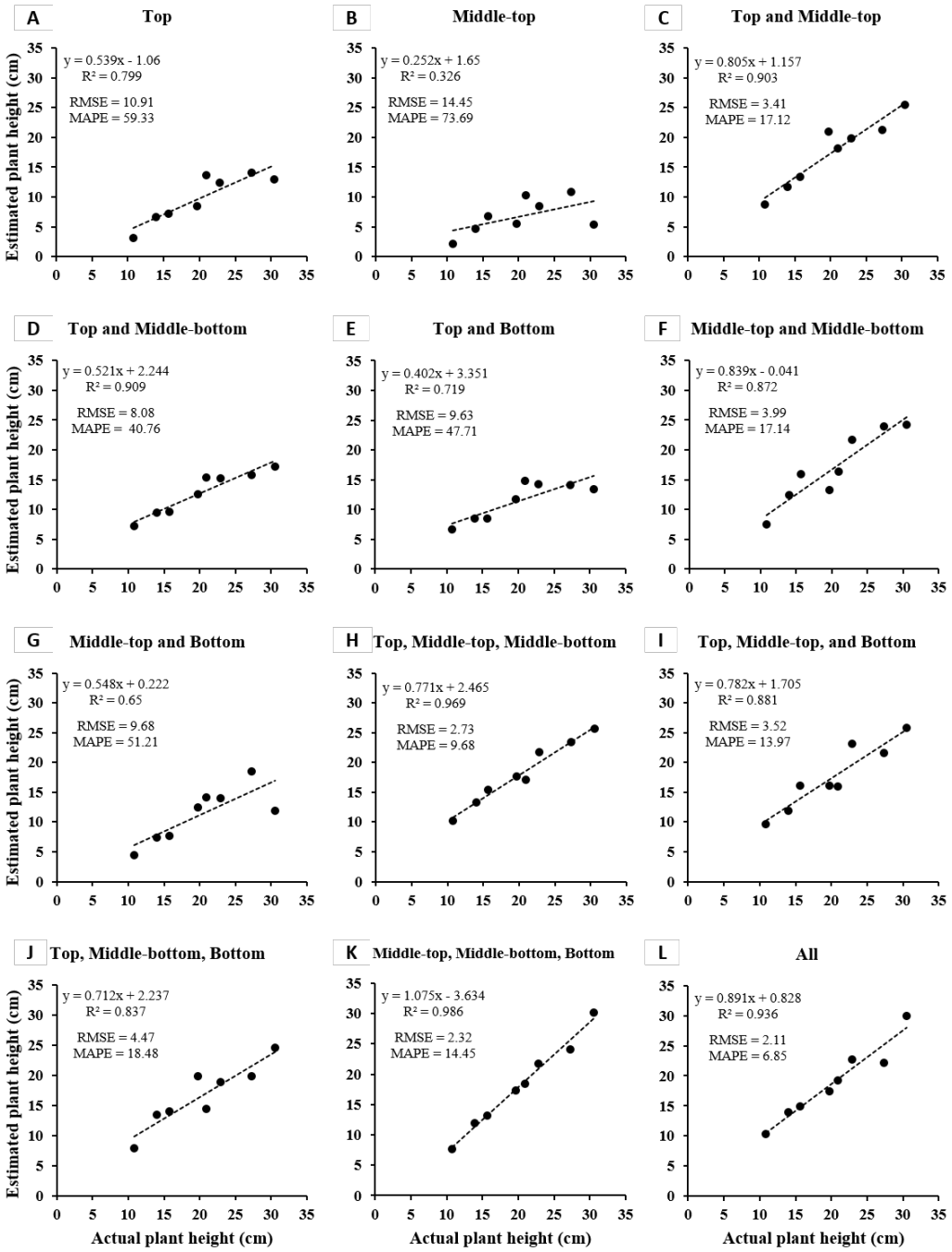

Fig 4. Validation results for the plant height parameters extracted using the UC Davis phenotyping system compared with the actual measurements using 12 different sets of camera viewpoints: (A) Top, (B) MT, (C) Top+MT, (D) Top+MB, (E) Top+Bottom, (F) MT+MB, (G) MT+Bottom, (H) Top+MT+MB, (I) Top+MT+Bottom, (J) Top+MB+Bottom, (K) MT+MB+Bottom, (L) All.

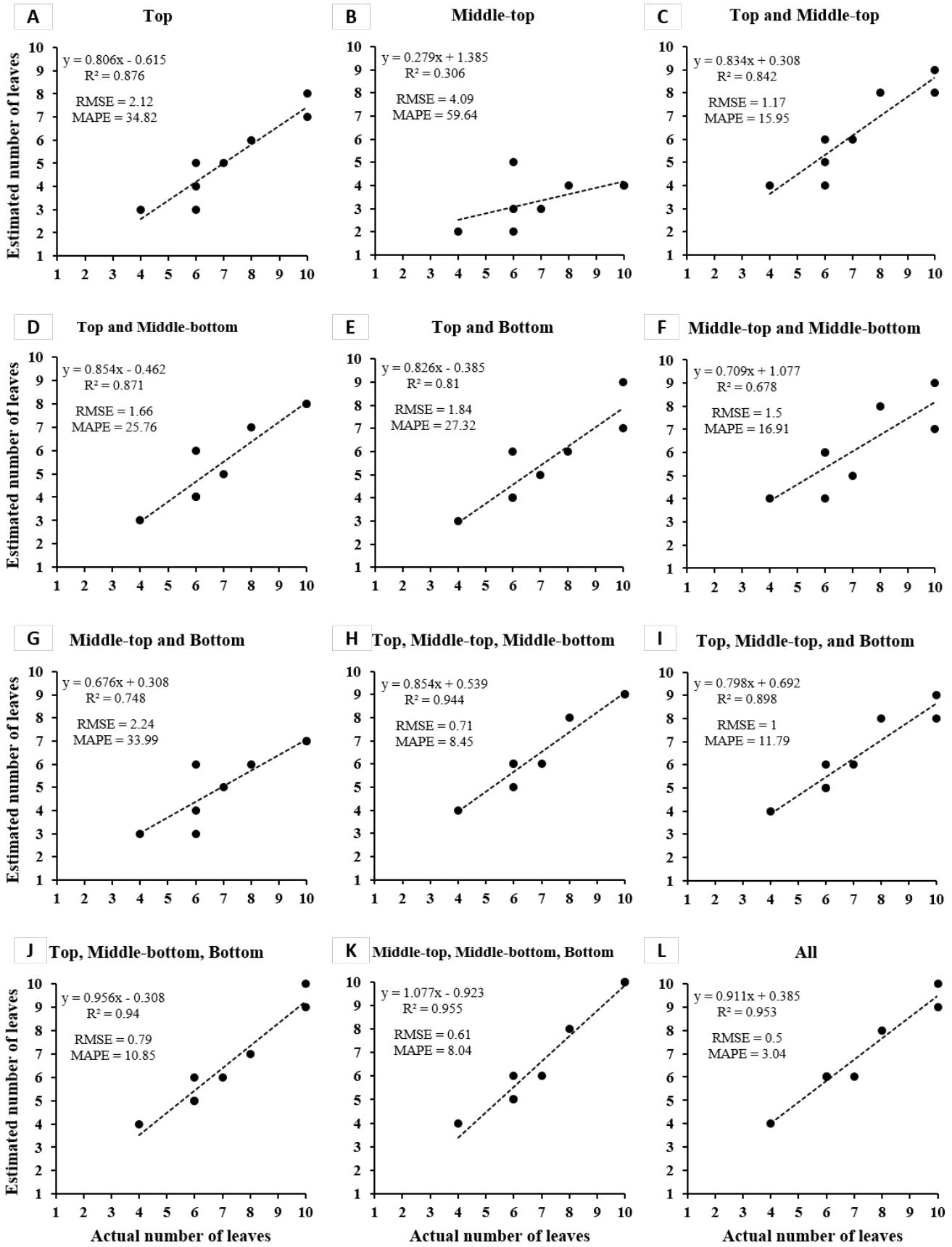

Fig 5. Validation results for the number of leaves phenotype extracted using the UC Davis phenotyping system compared with the actual measurements using 12 different sets of camera viewpoints: (A) Top, (B) MT, (C) Top+MT, (D) Top+MB, (E) Top+Bottom, (F) MT+MB, (G) MT+Bottom, (H) Top+MT+MB, (I) Top+MT+Bottom, (J) Top+MB+Bottom, (K) MT+MB+Bottom, (L) All.

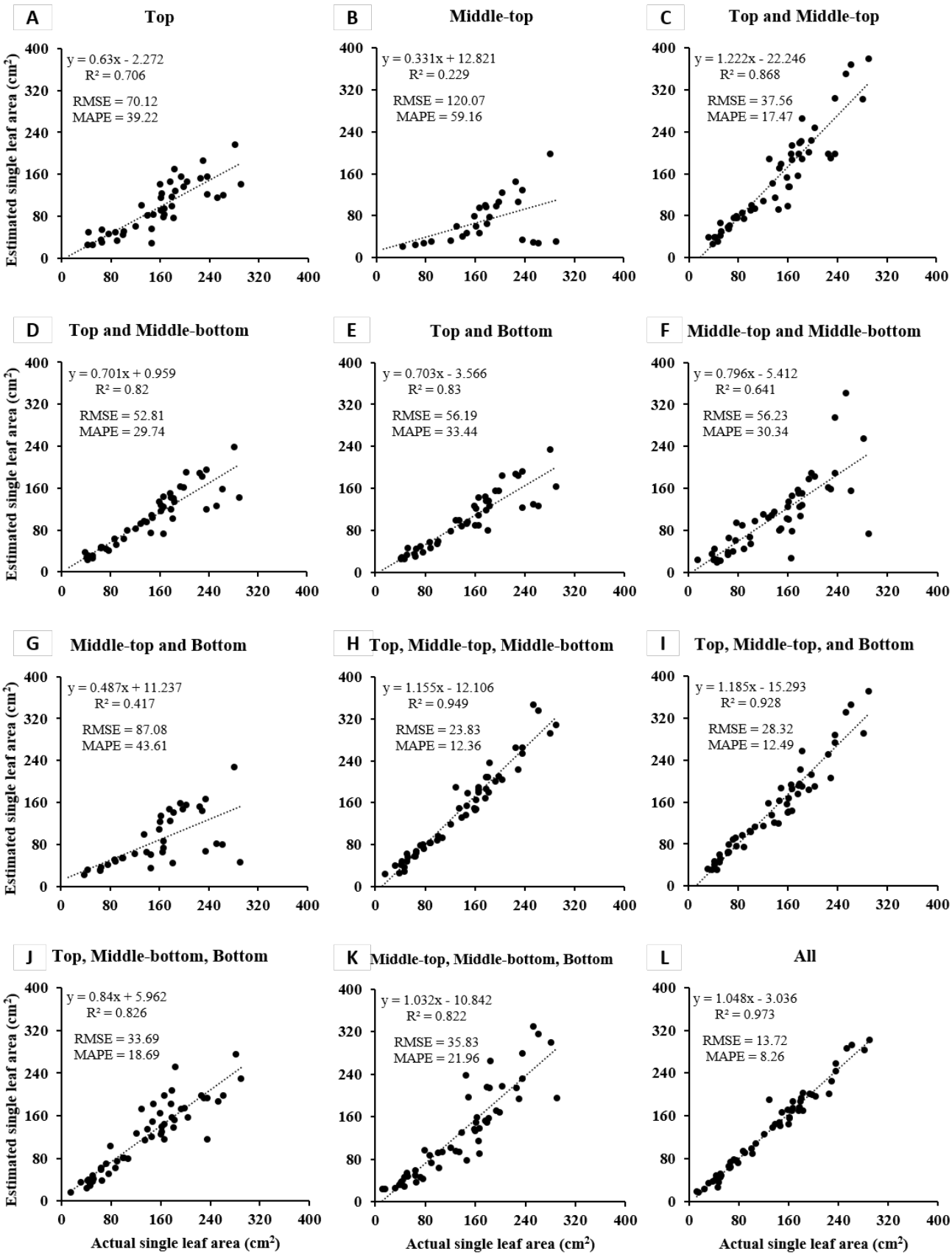

Fig 6. Validation results for the single leaf area phenotype extracted using the UC Davis phenotyping system compared with the actual measurements using 12 different sets of camera viewpoints: (A) Top, (B) MT, (C) Top+MT, (D) Top+MB, (E) Top+Bottom, (F) MT+MB, (G) MT+Bottom, (H) Top+MT+MB, (I) Top+MT+Bottom, (J) Top+MB+Bottom, (K) MT+MB+Bottom,

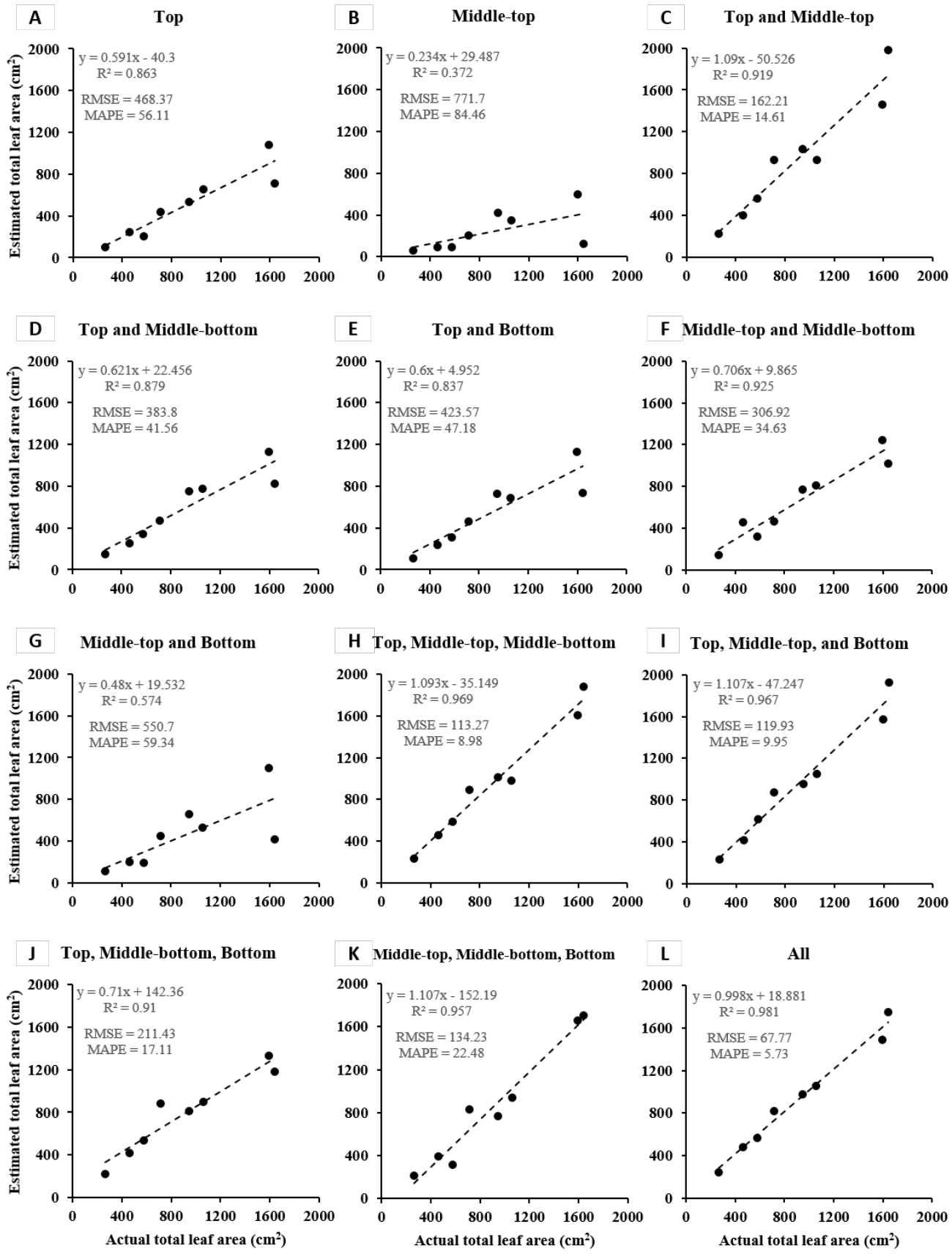

Fig 7. Validation results for the total leaf area phenotype extracted using the UC Davis phenotyping system compared with the actual measurements using 12 different sets of camera viewpoints: (A) Top, (B) MT, (C) Top+MT, (D) Top+MB, (E) Top+Bottom, (F) MT+MB, (G) MT+Bottom, (H) Top+MT+MB, (I) Top+MT+Bottom, (J) Top+MB+Bottom, (K) MT+MB+Bottom, (L) All.

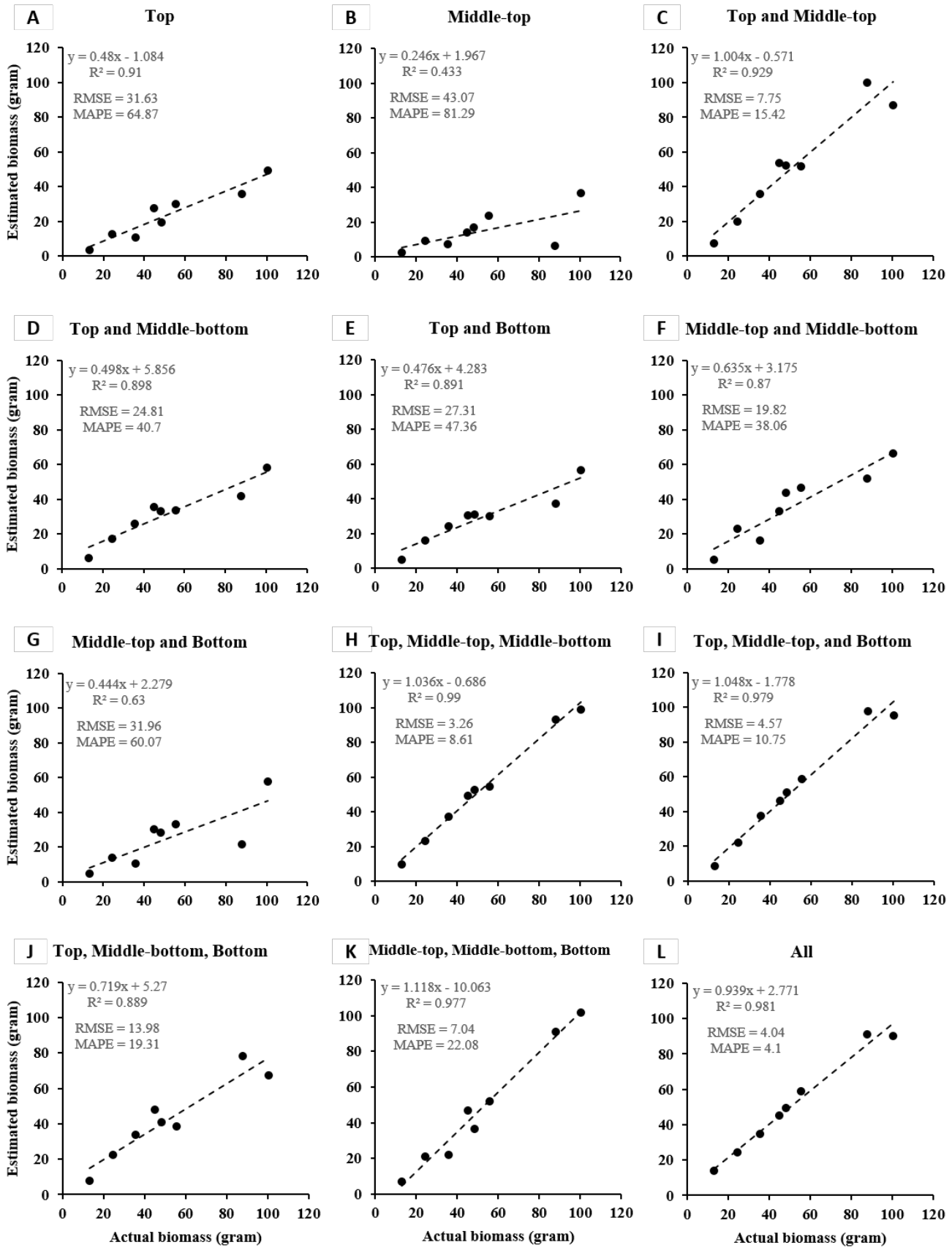

Fig 8. . Validation results for the plant biomass phenotype extracted using the UC Davis phenotyping system compared with the actual measurements using 12 different sets of camera viewpoints: (A) Top, (B) MT, (C) Top+MT, (D) Top+MB, (E) Top+Bottom, (F) MT+MB, (G) MT+Bottom, (H) Top+MT+MB, (I) Top+MT+Bottom, (J) Top+MB+Bottom, (K) MT+MB+Bottom, (L) All.

In general, the analysis showed that plant height, number of leaves, single leaf area, total leaf area, and plant biomass were well estimated in the *All* set where the cameras were located in positions surrounding the plant, indicating the potential of the camera positioning (to have the minimum number of cameras and optimized image overlapping) for plant phenotyping. The *MT+MB+B* and *T+MT+MB* sets had comparable performance to the *All* set. This indicates that with twelve well-positioned cameras, full 3D reconstruction and structure of a plant could be estimated satisfactorily. The results also indicated that camera positions were a key factor in successful plant phenotyping. Furthermore, side cameras (i.e. middle-bottom and bottom) used separately were not able to capture full plant features if they were not utilized together with the top cameras (i.e. middle-top and top). The use of top cameras did not only support the other ones, but also could be used independently for simple plants.

Due to the high resolution of our camera system (3 pixels per 1 mm), a single eggplant could be represented by up to 500,000 points (a single leaf could be up to 90,000 points), depending on its size. In comparison to the laser scanning system [Paulus 2014] and the single-camera system [Frasson 2010], which used up to 12,000 and 150 points to represent a leaf, a massive increase in imaging resolution was demonstrated in this study. For the minimum number of views, i.e. the top or *MT* set had four views, the reconstructed 3D model had up to 150,000 and 35,000 points for a single plant and leaf, respectively. This allowed more detail, smoother structures, and more accurate plant phenotyping even though a smaller number of camera views was utilized. Table 2 summarizes and compares this study to the study [Andujar 2015] in terms of system configuration, number of views for data evaluation, and plant feature extraction. Comparing the two studies highlights the advantages and disadvantages of this system design.

Table 2. Comparison of two data evaluation systems for plant phenotyping in different camera viewing angels.

	The study [Andujar 2015]	Our study
Sensor	Microsoft Kinect for Windows 1.0	Canon EOS Rebel T3
Image resolution	640 × 480	4272 × 2848
Number of views for evaluation	4 (top, downward, front, and upward view)	16 (all-around views)
Environment	In-field	In-field
Supported plant height	0.8 to 2 meters	0 to 0.65 meters
Target plant	Populus	Eggplant
Plant features	Leaf biomass, branch biomass, leaf area, plant biomass	Plant height, number of leaves, leaf area, plant biomass

Using a sufficient number of cameras and optimized image overlap (by well positioning the cameras), the validation of camera-based plant height, leaf area, and plant biomass for a plant growing outdoors in the field was proved to be credible. From the results of the All set, plant height was estimated with R^2 0.936, RMSE 2.11, MAPE 6.85; number of leaves was R^2 0.953, RMSE 0.5, MAPE 3.04; single leaf area was R^2 0.973, RMSE 13.72, MAPE 8.26; total leaf area was R^2 0.981, RMSE 67.77, MAPE 5.73; and plant biomass was R^2 0.981, RMSE 4.04, MAPE 4.1.

Increasing the complexity of plant structure, with increased plant age, increased the occlusion of plant parts, when the plant was photographed from one camera view. By incorporating side and top views efficiently, it was possible to generate accurate 3D point clouds (from 4, 8, 12, and 16 images taken in different views) with low occlusion percentages. This allowed small leaves at the bottom to be detected and characterized successfully even though they were occluded by big leaves when viewed from the top. Further, plant main stem was satisfactorily reconstructed to yield accurate plant height estimation.

The in-field applicability, non-invasive mode, high accuracy, and multiple parameter extraction from a single image set make this system appropriate for in-field high-precision plant phenotyping. To further advance high-throughput phenotyping, the software algorithms are required to be fully automated in the field. In the current work, these tasks were executed offline on a computer with parameter adjustment and optimization required for each type of plant.

Conclusions

A multi-view digital imaging system for 3D based plant phenotyping was successfully designed and evaluated using different camera viewing angles. Sixteen high-resolution color cameras were used in the system and were grouped into four sets of different height levels for data evaluation purpose: top (at an angle of 80° and a height of 130 cm relative the ground plane), middle-top (60°, 110 cm), middle-bottom (40°, 90 cm), and bottom (20°, 70 cm). The cameras were mounted on four arc superstructures designed for field deployment, four cameras per arc, at 0°, 90°, 180°, and 270°, respectively. This study presented the potential of using a minimum number of cameras with optimized image overlap to have a successful full 3D plant model. It was shown that there were no specifically best locations, except the top views were the best to connect other views and to have full surface information of top leaves, because plant parts were distributed in different directions and orientations. Top views were found most advantageous for small plants, while the side views provide greater information content for larger plants, where top views are detrimental in estimating plant height due to plant main stem occlusion by top leaves. Furthermore, leaf position relative to the cameras and leaf density were the key parameters to allocate the side cameras in certain positions and angles.

Acknowledgements

This work was supported in part by the USDA National Institute of Food and Agriculture Hatch/Multistate project CA-D-BAE-7808-RR and by the Research Investment in the Sciences and Engineering (RISE) program at the University of California, Davis, USA. Any opinions, findings, conclusions, or recommendations expressed in this publication are those of the author(s) and do not necessarily reflect the view of the National Institute of Food and Agriculture (NIFA) or the United States Department of Agriculture (USDA). The authors would like to thank Jedediah Roach, Loan-Anh Nguyen, Burt Vannucci, Leland Neilson, and Andy Cobb, Department of Biological and Agricultural Engineering, University of California, Davis, who helped build the system.

References

Dhondt, S., Wuyts, N., & Inze, D. (2013). Cell to whole-plant phenotyping: The best is yet to come. *Trends Plant Sci.*, 18, 428–439.

Furbank, R. T., & Tester, M. (2011). Phenomics-technologies to relieve the phenotyping bottleneck. *Trends Plant Sci.*, 16, 635–644.

Song, S., Glasbey, C. A., Horgan, G. W., Polder, G., Dieleman, J. A., & van der Heijden, G. W. A. M. (2014). Automatic fruit recognition and counting from multiple images. *Biosystem Engineering,* 118, 203–215.

Slaughter, D. C., Giles, D. K., & Downey, D. (2006). Autonomous robotic weed control systems: A review. *Computers and Electronics in Agriculture*, 61, 63–78.

Nguyen, T. T., Slaughter, D. C., Max, N., Maloof, J. N., & Sinha, N. (2015). Structured light-based 3D reconstruction system for plants. *Sensors*, 15(8), 18587–18612.

Nguyen, T. T., Slaughter, D. C., Hanson, B. D., Barber, A., Freitas, A., Robles, D., & Whelan, E. (2015). Automated mobile system for accurate outdoor tree crop enumeration using an uncalibrated camera. *Sensors*, 15(8), 18427–18442.

Grift, T. E., Novais, J., & Bohn, M. (2011). High-throughput phenotyping technology for maize roots. *Biosystem Engineering*, 110, 40–48.

Song, S., Glasbey, C. A., Polder, G., & van der Heijden, G. W. A. M. (2014). Nondestructive automatic leaf area measurements by combining stereo and time-of-flight images, *IET Comput. Vis.*, 8(5), 391–403.

Paproki, A., Sirault, X., Berry, S., Furbank, R., & Fripp, J. (2012). A novel mesh processing based technique for 3D plant analysis. *BMC Plant Biol.*, 12, 1–13.

Baumberg, A., Lyons, A., & Taylor, R. (2005). 3D S.O.M.–A commercial software solution to 3D scanning. *Graph. Models*, 67, 476–495.

Chene, Y., Rousseau, D., Lucidarme, P., Bertheloot, J., Caffier, V., Morel, P., Belin, E., & Chapeau-Blondeau, F. (2012). On the use of depth camera for 3D phenotyping of entire plants. *Comput. Electron. Agric.*, 82 (2012) 122–127.

Zhang, Z. (2012). Microsoft Kinect sensor and its effect. *IEEE Multimedia*, 19, 4–12.

Heijden, G., Song, Y., Horgan, G., Polder, G., Dieleman, A., Bink, M., Palloix, A., Eeuwijk, F., & Glasbey, C. (2012). SPICY: Towards automated phenotyping of large pepper plants in the greenhouse. *Funct. Plant Biol.*, 39, 870–877.

Rose, J. C., Paulus, S., & Kuhlmann, H. (2015). Accuracy analysis of a multi-view stereo approach for phenotyping of tomato plants at the organ level. *Sensors*, 15, 9651–9665.

Andujar, D., Fernandez-Quintanilla, C., & Dorado, J. (2015). Matching the best viewing angle in depth cameras for biomass estimation based on poplar seedling geometry. *Sensors*, 15, 12999–13011.

Koutsoudis, A., Vidmar, B., Ioannakis, G., Arnaoutoglou, F., Pavlidis, G., & Chamzas, C. (2014). Multi-image 3D reconstruction data evaluation. *J. Cult. Herit.*, 15, 73–79.

Nguyen, T. T., Slaughter, D. C., Maloof, J. N., & Sinha, N. (2016). Plant phenotyping using multi-view stereo vision with structured lights. In Proceedings of the Autonomous Air and Ground Sensing Systems for Agricultural Optimization and Phenotyping Conference. Baltimore, Maryland, USA.

Nguyen, T. T., Slaughter, D. C., Townsley, B., Carriedo, L., Maloof, J. N., & Sinha, N. (2016). Comparison of structure-from-motion and stereo vision techniques for full in-field 3D reconstruction and phenotyping of plants: An investigation in sunflower. In Proceedings of the ASABE Annual International Meeting. Orlando, Florida, USA.

Agisoft Photoscan. http://www.agisoft.com (2016).

Rusu, R. B. (2009). Semantic 3D object maps for everyday manipulation in human living environments. *Ph.D. thesis*, *Computer Science Department*, *Technische Universitaet Muenchen*, Germany.

Paulus, S., Schumann, H., Kuhlmann, H., & Leon, J. (2014). High-precision laser scanning system for capturing 3D plant architecture and analysing growth of cereal plants. *Biosystem Engineering*, 121, 1–11.

Calders, K., Newnham, G., Burt, A., Murphy, S., Raumonen, P., Herold, M., Culvenor, D., Avitabile, V., Disney, M., Armston, J., & Kaasalainen, M. (2015). Nondestructive estimates of above-ground biomass using terrestrial laser scanning. *Methods Ecol. Evol.*, 6, 198–208.

Costes, E., Smith, C., Renton, M., Guedon, Y., Prusinkiewicz, P., & Godin, C. (2008) MAppleT: Simulation of apple tree development using mixed stochastic and biomechanical models. *Funct. Plant Biol.*, 35, 936–950.

Paul, K. I., Roxburgh, S. H., England, J. R., Ritson, P., Hobbs, T., Brooksbank, K., Raison, R. J., Larmour, J. S., Murphy, S., Norris, J., Neumann, C., Lewis, T., Jonson, J., Carter, J. L., McAuthur, G., & Barton, C. (2013). Development and testing of allometric equations for estimating above-ground biomass of mixed-species environmental plantings. *Forest Ecol. Manag.*, 35, 483–494.

GIMP – GNU Image Manipulation Program. http://www.gimp.org (2016).

ImageJ. http://rsb.info.nih.gov/ij (2016).

Frasson, R. P. D., & Krajewski, W. F. (2010). Three-dimensional digital model of a maize plant. *Agr. Forest. Meteorol.,* 150, 478–488.